NASA TECHNICAL
MEMORANDUM

NASA TM X-3155

NASA TM X-3155

HIGH-PERFORMANCE AUXILIARY-PROPULSION ION THRUSTER WITH ION-MACHINED ACCELERATOR GRID

Wayne R. Hudson and Bruce A. Banks

Lewis Research Center
Cleveland, Ohio 44135

NATIONAL AERONAUTICS AND SPACE ADMINISTRATION • WASHINGTON, D. C. • JANUARY 1975

1. Report No. NASA TM X-3155	2. Government Accession No.	3. Recipient's Catalog No.
4. Title and Subtitle HIGH-PERFORMANCE AUXILIARY-PROPULSION ION THRUSTER WITH ION-MACHINED ACCELERATOR GRID		5. Report Date January 1975
		6. Performing Organization Code
7. Author(s) Wayne R. Hudson and Bruce A. Banks		8. Performing Organization Report No. E-8078
9. Performing Organization Name and Address Lewis Research Center National Aeronautics and Space Administration Cleveland, Ohio 44135		10. Work Unit No. 506-22
		11. Contract or Grant No.
12. Sponsoring Agency Name and Address National Aeronautics and Space Administration Washington, D.C. 20546		13. Type of Report and Period Covered Technical Memorandum
		14. Sponsoring Agency Code

15. Supplementary Notes

16. Abstract

A substantial improvement in thruster performance has been achieved by reducing the diameter of the accelerator grid holes. The smaller accelerator grid holes resulted in a reduction in neutral mercury atoms escaping the discharge chamber, which in turn enhanced the discharge propellant utilization from approximately 68 percent to 92 percent. The accelerator grids were fabricated by ion machining with an 8-centimeter-diameter thruster. The screen grid holes individually focused ion beamlets onto the blank accelerator grid. The resulting accelerator grid holes are less than 1.12 millimeters in diameter. Previously used accelerator grids had hole diameters of 1.69 millimeters. The thruster could be operated with the small-hole accelerator grid at neutralizer potential.

17. Key Words (Suggested by Author(s)) Electron bombardment thruster Auxiliary propulsion Ion machining	18. Distribution Statement Unclassified - unlimited STAR category 28		
19. Security Classif. (of this report) Unclassified	20. Security Classif. (of this page) Unclassified	21. No. of Pages 24	22. Price* $3.00

HIGH-PERFORMANCE AUXILIARY-PROPULSION ION THRUSTER

WITH ION-MACHINED ACCELERATOR GRID

by Wayne R. Hudson and Bruce A. Banks

Lewis Research Center

SUMMARY

A substantial improvement in thruster performance has been achieved by reducing the diameter of the accelerator grid holes. The smaller accelerator grid holes resulted in a reduction in neutral mercury atoms escaping the discharge chamber, which in turn enchanced the discharge propellant utilization from approximately 68 percent to 92 percent. The accelerator grids were fabricated by ion machining with an 8-centimeter-diameter thruster. The screen grid holes individually focused ion beamlets onto the blank accelerator grid. The resulting accelerator grid holes are less than 1.12 millimeters in diameter. Previously used accelerator grids had hole diameters of 1.69 millimeters. The thruster could be operated with the small-hole accelerator grid at neutralizer potential.

INTRODUCTION

The Lewis Research Center auxiliary electric propulsion program is currently developing an 8-centimeter-diameter electron bombardment ion thruster for stationkeeping and attitude control applications.

The thruster system has a design life of 20 000 hours and 10 000 on-off cycles at a 3000-second specific impulse and a 4.5-millinewton thrust. The thruster employs a two-grid ion extraction system consisting of two dished grids with matched hexagonal arrays of holes. The grids are fabricated from arc-cast molybdenum sheet by photo-chemical etching and hydroforming (ref. 1).

This report describes a high-performance auxiliary propulsion ion thruster which has resulted from a unique new grid fabrication technique. The screen and accelerator grid are simultaneously hydroformed as before, but only the screen grid hole array is etched. The accelerator grid is initially unperforated. The grid set is then mounted on

a thruster in the usual manner. The screen electrode focuses individual ion beamlets onto the blank accelerator grid, selectively sputtering a matching array of holes in the accelerator grid. The resulting accelerator grid holes are sized, shaped, and alined with respect to their corresponding screen holes. The accelerator holes are much smaller than previously used accelerator grid holes, thereby reducing the neutral mercury loss. As a result, propellant utilization is enhanced (as is consistent with trends documented by Rawlin, refs. 2 and 3).

A thruster with an ion-machined grid has been tested for 1006 hours at an ion chamber propellant utilization of 91.9 percent and at discharge losses of less than 350 eV/ion. This represents a substantial increase in propellant utilization (previously 68.3 percent) over thrusters operated with larger-hole-diameter accelerator grids.

APPARATUS AND PROCEDURE

For both the ion machining process and the subsequent thruster operation, the vacuum facility employed was 4.5 meters long by 1.5 meters in diameter. The thruster test chamber was connected to the facility through a 0.3-meter gate valve. The facility was maintained at 10^{-6} torr during thruster operation.

The 8-centimeter-diameter thruster used is shown in cross section in figure 1. The thruster had a cylindrical shell engine body 9.3 centimeters in diameter and a concentric anode 8.4 centimeters in diameter. Six 0.635-centimeter-diameter permanent magnets were distributed evenly around the engine body circumference, a screen pole piece was in the proximity of the beam extraction system, and a cathode pole piece surrounded the cathode. The cathode pole piece was conical design 1.65 centimeters in height and 1.58 centimeters in inside diameter. The tantalum baffle itself was 0.635 centimeter in diameter and was mounted in the plane of the downstream edge of the cathode pole piece by three support wires. The screen pole piece had a cylindrical collar 1.12 centimeters long and a truncated conical surface 0.71 centimeter long which formed a 20° angle with respect to the thruster axis. The smallest diameter of the screen pole piece was 8.4 centimeters. The main cathode and the neutralizer were both enclosed-keeper hollow cathodes, described in detail in reference 1. The cathode and neutralizer had 0.25-millimeter orifices in the cathode tip. The cathode had a 2.5-millimeter-diameter keeper orifice. The neutralizer keeper orifice was 1.14 millimeters. Mercury flow measurements were determined by measuring the time rate of change of mercury level in a precision 0.5-millimeter-diameter burette. The screen and accelerator grid were both hydroformed to a depth of 0.25 centimeter, which corresponds to a radius of curvature of 30 centimeters. The screen grid was 0.40 milli-

meter thick and had an open area of 72.5 percent (1.97-mm-diam holes on 2.21 mm centers). The accelerator grid was unperforated molybdenum sheet 0.38 millimeter thick. The screen and blank accelerator grid were mounted to provide a uniform intergrid gap of 0.76 millimeter. The gap between grids was intentionally made larger than usual to minimize intergrid shorting during the machining process.

The electrical circuit shown in figure 2 was used to operate the thruster during ion machining and normal thruster operation. The anode was held at the net accelerating voltage V_I. The cathode was negatively biased by the discharge chamber supply, and the neutralizer floating potential was measured between the neutralizer tip and the facility ground. There were only two differences between the power supplies and circuit used in this experiment and the normal thruster electrical circuit: a 4-microfarad capacitor was connected in parallel between the accelerator grid and the cathode common, and an accelerator supply was used that had a current capability of 100 milliamperes. The purpose of the capacitor was to prevent flakes of sputtered material from permanently shorting the grids together. When a flake shorted the grids, the capacitor discharged through the flake thereby vaporizing it. The extra current capacity of the accelerator supply was necessary because in the initial stages of the machining operation the accelerator supply must carry the full ion beam current.

At the start of the ion machining process, it was necessary to reduce the mercury flow to a few equivalent milliamperes because the initially unperforated accelerator grid prevented the normal ion and neutral propellant loss from the discharge chamber. The mercury flow was regulated such that the discharge voltage was above 30 volts. Later, as the ion beamlets sputtered through the accelerator grid, the mercury flow was gradually increased to the normal levels.

Because the thruster beam current J_B was measured as the current drawn by the neutralizer (fig. 2), it read zero as long as there were no holes sputtered through the accelerator grid. The total ion current was indicated as accelerator current J_A and as net-accelerating-potential supply current J_B', where $J_B' = J_B + J_A$. These three currents served as convenient parameters for monitoring the machining process. Initially, J_B equaled zero and J_B' equaled J_A, but as the holes began to machine through the accelerator grid J_B started increasing and J_A started decreasing. The relative magnitudes of J_B and J_A are sensitive indicators of the progress of the ion machining. Starting with a blank accelerator grid, J_B increased from zero to the full beam current (72 mA) and J_A decreased from the full beam current to its equilibrium level.

After 2 hours of ion beam operation, holes began to sputter through the 0.38-millimeter-thick accelerator grid. As might be expected, the first breakthrough occurred in the center of the accelerator grid. The time of breakthrough was denoted by an increase in J_B and a decrease in J_A. Figure 3 is a plot of both normalized accelerator current J_A/J_B' and normalized beam current J_B/J_B'. The accelerator hole breakthrough point is marked as AA'. During the 2-hour period from AA' to BB',

3

J_B' was held at 72 milliamperes, and the discharge voltage ΔV_I was maintained between 30 and 40 volts by gradually increasing the mercury flow rate. The net accelerator voltage V_I was held at 1220 volts, and the accelerator voltage V_A was maintained at -300 volts. At BB', J_B/J_B' had increased to 0.75 and J_A/J_B' had decreased to 0.23. The thruster was examined at this point, and a photographic record of the accelerator grid condition was made.

When the test was restarted at BB', several changes were made in an effort to increase the ion machining rate. The beamlets were broadened by increasing V_A to -500 volts. The mercury flow rate was also increased consistent with maximizing J_B'. The limit of the V_I supply was 100 milliamperes. These changes in operating conditions did cause an increase in J_A/J_B' that can be noted at point BB' in figure 3. Points CC', DD', and EE' indicate times at which the thruster was shut down overnight. At point EE', after less than 14 hours, both J_A and J_B were becoming relatively constant. Thruster beam current J_B was essentially equal to J_B'. Accelerator current J_A was reduced to 3 percent of its original value, but it still was 10 times normal J_A levels.

From this point, the accelerator current continued to decrease, but very slowly. Figure 4 gives the variation of J_A over 1000 hours of operation. Even after 400 hours, J_A was still 75 percent greater than the J_A levels normally achieved. After 1000 hours, J_A reached 0.25 milliampere, which was still 25 percent greater than the normal level (0.20 mA). The slow continual decrease was probably caused partially by erosion of the thick grid mounting ring by defocused beamlets from partially blocked holes at the outer edge of the screen grid.

During the early stages of the ion machining process, frequent grid short circuits were observed (estimated at one every 5 sec). The short circuits were caused by flakes of sputtered material and were all eliminated by the capacitor discharge. In order to maintain continuity of thruster operation, the cathode and neutralizer were operated at high levels of tip heat ($>$30 W). This ensured that cathodes could be reignited automatically after outages due to electrical transients resulting from grid short circuits. Both the cathode and neutralizer inserts suffered from performance deterioration resulting from this abnormal mode of operation.

RESULTS AND DISCUSSION

Accelerator Grid

The upstream and downstream faces of the grid assembly after 1006 hours of operation are shown in figure 5. Measurements of the accelerator grid hole diameter were made from photomicrographs of several positions on both sides of the grid.

Accelerator grid hole diameter measurements at five different times and at four locations are listed in table I.

Because of higher beam density in the center of the grid, ion machining occurred at a faster rate there. After 4 hours, accelerator holes were sputtered through in the center, but not at the outer edges of the grid. Figure 6 is a photomicrograph of a downstream view of the accelerator grid after 4 hours of ion machining. A variation in hole diameter can be noted. A few of the holes were just barely ion machined through, and part of the accelerator grid is shown where holes were not yet sputtered through. Photomicrographs of partially sputtered-through accelerator holes as viewed from the downstream side are shown in figure 7. Upstream views of the partially ion-machined region of the accelerator grid are presented in figure 8. On the left is a low-magnification view of a region where some of the holes were ion machined all the way through and others were only partially through the 0.38-millimeter-thick accelerator. The accelerator and screen grid remained mounted on the grid assembly during photographing, and as a consequence the upstream photographs include the screen grid. On the right in figure 8 is a high-magnification view of one particular accelerator hole, showing the upstream and downstream perimeters of the hole. The individual beamlets appear to be focusing at a point downstream of the accelerator grid.

Table I shows the time variation of the hole diameters at four different positions on the accelerator grid. At some locations the machining process achieved the equilibrium hole diameter and at some it did not.

Near the outer edges of the accelerator grid the ion machining process was slower and more complex in structure. Measurements indicated that on the downstream side the edge holes increased in size throughout the test but that on the upstream side they stabilized after 462 hours. On the upstream side of the accelerator grid the holes were circular, but on the downstream side of the accelerator grid the holes more closely approximated hexagons. Figure 9 (top) is a photomicrograph of several holes after 462 hours of ion machining. The hexagonal pattern appears to be a result of the screen hole array pattern. The sides of a particular hexagon are roughly perpendicular to lines connecting the center of the hexagon to its nearest neighbors. Figures 9 (bottom) is a higher magnification photomicrograph of an accelerator hole.

At the end of the 1000-hour test it was noted that on the downstream side of the accelerator grid the holes midway between the center of the grid and the edge were smaller than the holes at the edge. Measurements showed that the hole diameter at the midway point was 0.74 millimeter on the downstream side, which is smaller than the hole diameter at the edge. Measurements were also made of the hole diameter midway to the center on the upstream surface of the accelerator grid. In this case the diameter was measured to be 0.94 millimeter, which is intermediate to center-hole diameter and edge-hole diameter.

Charge exchange erosion was observed on the downstream side of the accelerator grid (fig. 10). The darker-colored hexagon web structure is the region that has been sputtered by charge exchange ions. The charge exchange pattern was most intense in the center of the grid.

The accelerator grid and screen grids were held in place by a pair of mounting rings. The accelerator grid mounting ring was sputtered by ion beamlets from partially covered screen holes. The accelerator current and the sputtered mounting ring material resulting from this erosion should be avoided. This could be achieved by eliminating partial holes from the screen grid. Figure 11 is a photomicrograph of the sputtered grooves in the accelerator grid mounting ring.

In some cases, accelerator grid material sputtered onto the inside of the screen holes. Photomicrographs of two specific examples are shown in figure 12. These photographs were taken after 20 hours. As would be expected, the fastest rate of deposit occurred during the first few hours. In some cases the deposited material spalled, partially blocking the screen hole and defocusing the ion beamlet. Two examples of distorted accelerator grid holes are shown in figure 13. There were only seven distorted holes. This effect could be eliminated by more frequent cleaning during the early stages of ion machining. The grid system was cleaned of sputtered material five times over the 1000 hours of this test. Although no permanent short circuits resulted, more inspections and cleanings, especially early in the machining process, are recommended. The screen grid deposits were sandblasted away after 149 hours. Subsequent inspections did not reveal additional deposits.

Thruster Performance

The accelerator holes resulting from the ion machining process are optimally sized to the ion beamlets. The smaller accelerator holes result in reduced neutral mercury loss, which in turn enhances the propellant utilization.

The propellant utilization η_u is equal to the ratio of beam current to total mercury flow

$$\eta_u = \frac{J_B}{J_B + J_N} \tag{1}$$

where J_N is equal to the un-ionized part of the total mercury flow. If it is assumed that the neutral loss rate from the discharge chamber is proportional to the open area of the accelerator grid,

$$\frac{J_{N1}}{J_{N2}} = \frac{A_1}{A_2} = \frac{D_1^2}{D_2^2} \tag{2}$$

where A_1 and A_2 are two different open areas and D_1 and D_2 are the corresponding accelerator hole diameters. Then given empirical results of a particular accelerator hole diameter, a relation can be derived for the approximate propellant utilization as a function of accelerator hole diameter. For $D_1 = 1.69$ millimeters and $J_B = 72$ milliamperes, thrusters have operated at 70 perce..t propellant utilization, at discharge losses of 300 to 350 eV/ion. From equation (1) J_{N1} can be calculated to be 30.8 milliamperes. Then using equations (1) and (2)

$$\eta_{u2} = \frac{J_B}{J_B + J_{N1}\left(\dfrac{D_2^2}{D_1^2}\right)} = \frac{1}{1 + \dfrac{J_{N1}}{J_B}\left(\dfrac{D_2^2}{D_1^2}\right)}$$

Substituting yields

$$\eta_u = \frac{1}{1 + 0.149\, D^2} \tag{3}$$

Figure 14 is a plot of propellant utilization as a function of accelerator hole diameter calculated from equation (3). Large increases in propellant utilization are predicted for small accelerator grid holes. The ion beamlet diameter represents a lower limit to the accelerator hole diameter. As demonstrated by the results of ion machining experiments, if the accelerator holes are smaller in diameter than the beamlet diameter, they will be enlarged by sputtering. The ion-machined accelerator grid geometry that results yields the maximum achievable propellant utilization efficiency.

The performance of an 8-centimeter-diameter thruster with an ion-machined accelerator grid can be compared with the predictions of figure 14. Because the hole diameter of the ion-machined accelerator grid varies with respect to hole location, a conservative choice is the accelerator grid hole diameter measured in the center of the grid on the downstream side. The upper limit listed in table I is 0.84 millimeter, which would predict a propellant utilization efficiency of 90 percent. This represents a lower limit on propellant utilization because many of the accelerator holes are considerably smaller.

The discharge power losses are plotted as a function of the discharge chamber propellant utilization in figure 15 for a thruster with an ion-machined accelerator grid, at 149 and 1006 hours, and the same thruster with a Large-Hole Accelerator Grid (LHAG).

The LHAG had a hole diameter of 1.69 millimeters. The Small-Hole Accelerator Grid (SHAG) that results from ion machining is clearly superior. It performs at lower discharge chamber losses and yet much higher propellant efficiencies. During most of the ion machining experiment the SHAG thruster was run at near 90 percent utilization and with discharge losses of 325 eV/ion. A complete set of SHAG thruster operating parameters is shown in table II. For comparison, the small-thruster program goals and the operating parameters of the LHAG thruster are listed. The SHAG thruster closely approximates the program goals. The small-thruster program goal for total efficiency is 57.5 percent, and the SHAG thruster operated at 56.7 percent.

The LHAG configured thruster was tested at two operating points. The first operating point was with the same mercury flow rate and discharge power as the SHAG thruster. The LHAG thruster produced a beam current of 59.8 milliamperes, which corresponds to a thrust of 4.18 millinewtons (0.94 mlb) at 465 eV/ion. The second test was with the mercury flow rate increased such that the thruster could produce a 72-milliampere beam current (5.07-mN (1.14-mlb) thrust). This point is listed in table II. A mercury flow rate of 106 milliamperes was required. Propellant utilization was below 70 percent, at 381 eV/ion. The lower propellant utilization decreased the specific impulse to 2247 seconds.

In figure 15, two curves are graphed for the SHAG thruster, one after 149 hours and one after 1006 hours. Comparison of the SHAG thruster curves reveals a 3 percent decrease in propellant utilization with time. It was probably a result of an increase in the diameter of the accelerator grid holes.

Figure 16 exhibits the accelerator current dependence on total voltage. Values are plotted for -300 volts and zero volts applied to the accelerator grid. The thruster operated satisfactorily with the accelerator supply set at zero volts (accelerator at neutralizer tip potential) if the net accelerating voltage was increased to maintain the same total voltage. With zero accelerator voltage the accelerator current was slightly less than with -300 volts applied to the accelerator grid. These results suggest the possibility of operating the thruster without an accelerator supply, which would result in weight savings to the thruster system. Perhaps electrically attaching the accelerator grid to the neutralizer tip potential would ensure enough of an electron backstreaming barrier even if the small accelerator holes were photoetched rather than ion machined. Certainly, accelerator grid lifetime would be greatly increased if the grid could operate near zero volts.

CONCLUDING REMARKS

The holes of an accelerator grid were ion machined by operating an 8-centimeter-diameter thruster with an initially unperforated accelerator grid. The resulting accel-

erator grid had a distribution of hole diameters all of which were much smaller than those previously tested. The ion machining process creates an ideally matched accelerator grid for a given thruster and thruster operating conditions.

The smaller holes in the accelerator grid resulted in an increase from 68.3 percent to 91.9 percent in ion chamber propellant utilization with no increase in discharge chamber power losses. The thruster was subsequently operated for over 1000 hours. Because the resulting accelerator holes were small, electron backstreaming would not occur even when the accelerator grid was operated with the accelerator supply shut off with the accelerator grid at neutralizer tip potential.

Lewis Research Center,
    National Aeronautics and Space Administration,
        Cleveland, Ohio, October 10, 1974,
            506-22.

REFERENCES

1. Danilowicz, Ronald L.; Rawlin, Vincent K.; Banks, Bruce A.; and Wintucky, Edwin G.: Measurement of Beam Divergence of 30-Centimeter Dished Grids. NASA TM X-68286, 1973.

2. Rawlin, Vincent K.: Studies of Dished Accelerator Grids for 30-Centimeter Ion Thrusters. NASA TM X-71420, 1973.

3. Rawlin, Vincent K.: Performance of 30-Centimeter Ion Thrusters with Dished Accelerator Grids. NASA TM X-68294, 1973.

TABLE I. - ACCELERATOR GRID HOLE DIAMETERS

Operating time, hr	Upstream side of grid		Downstream side of grid	
	Center-hole diameter, mm	Edge-hole diameter, mm	Center-hole diameter, mm	Edge-hole diameter, mm
4	0.68	(a)	0.47	(a)
20	.84	0.72	.61	[b]0.51 - 0.61
149	----	----	.83	[b]0.61 - 0.69
462	1.04	.86	.83	0.66 - 0.76
1006	1.12	.86	.83	0.71 - 0.82

[a]Not sputtered through.

[b]Hexagonal - smaller value is distance between opposite sides of hexagon; larger value is distance between opposite vertices of hexagon.

	Program goal	Small-hole accelerator grid conditions	Large-hole accelerator grid conditions
Thrust[a] (ideal), MN	5.07	5.16	5.16
Specific impulse,[a] sec	2804	2958	2247
Total input power, W	122.19	131.54	134.21
Total efficiency,[a] percent	57.5	56.7	42.2
Power efficiency, percent	71.3	66.4	65.3
Total utilization,[a] percent	80.6	85.4	64.6
Discharge utilization,[a] percent	86.4	91.9	68.3
Total neutral flow, mA	89.3	85.2	112.0
Power/thrust,[a] W/mN	24.10	24.49	26.00
Discharge loss excluding keeper voltage, eV/ion	294	286	369
Discharge loss including keeper voltage, eV/ion	328	338	381
Beam current, J_B, mA	72	72.8	72.4
Net accelerating voltage, V_I, V	1220	1220	1220
Neutralizer floating potential, V_g, V	-10	-20	-10
Output beam power, W	87.12	87.36	87.60
Accelerator voltage, V_A, V	-500	-300	-300
Accelerator drain current, J_A, mA	0.23	0.25	0.35
Accelerator drain power, W	0.40	0.38	0.53
Discharge voltage, ΔV_I, V	40	38.5	40.5
Emission current, J_E, A	0.53	0.54	0.66
Discharge power, W	21.2	20.79	26.73
Cathode:			
Keeper voltage, V_{CH}, V	10.0	17.5	16.5
Keeper current, J_{CK}, A	0.240	0.22	0.05
Keeper power, W	2.4	3.85	0.83
Heater voltage, V_{CH}, A	0	0	0
Heater current, J_{CH}, A	0	0	0
Heater power, W	0	0	0
Vaporizer voltage, V_{CV}, V	4.0	2.2	2.2
Vaporizer current, J_{CV}, A	1.0	2.1	2.1
Vaporizer power, W	4.0	4.6	4.6
Flow rate, mA	83.3	79.2	106.0
Neutralizer:			
Keeper voltage, V_{NK}, V	14.1	17.8	18.0
Keeper current, J_{NK}, A	0.360	0.5	0.5
Keeper power, W	5.08	8.9	9.0
Heater voltage, V_{NH}, V	0	0	0
Heater current, J_{NH}, A	0	0	0
Heater power, W	0	0	0
Vaporizer voltage, V_{NV}, V	1.65	2.1	2.1
Vaporizer current, J_{NV}, A	0.77	2.0	2.0
Vaporizer power, W	1.27	4.2	4.2
Flow rate, mA	6.0	6.0	6.0
Neutralizer coupling power, W	0.72	1.46	0.72

[a]Accounting for neutralizer floating potential but neglecting beam divergence and double ionization.
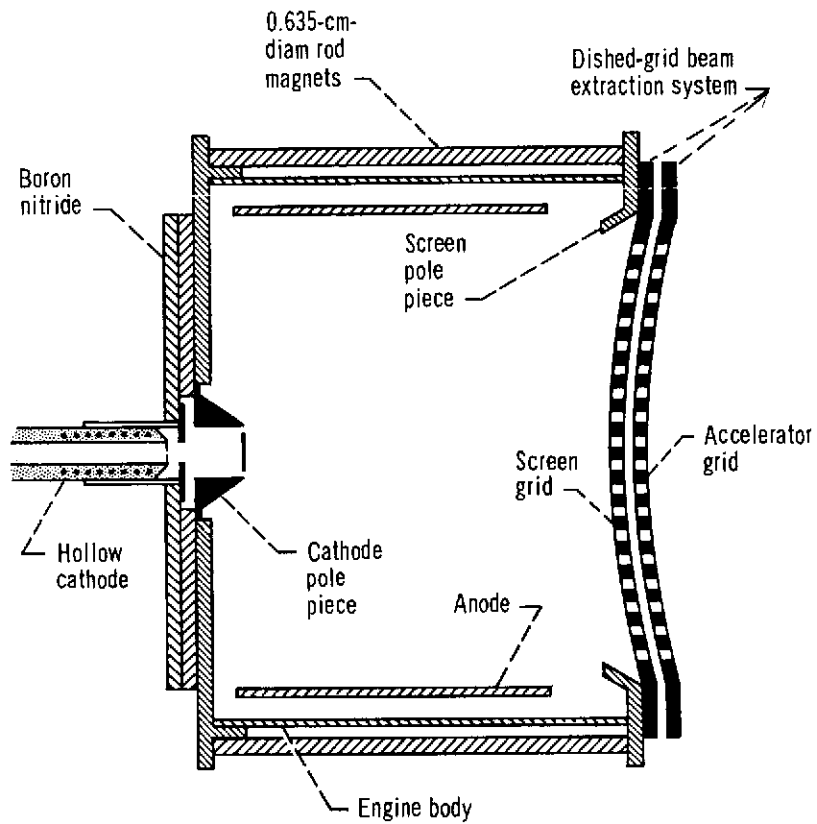
Figure 1. - Cross section of 8-centimeter-diameter thruster discharge chamber with dished-grid beam extraction system.
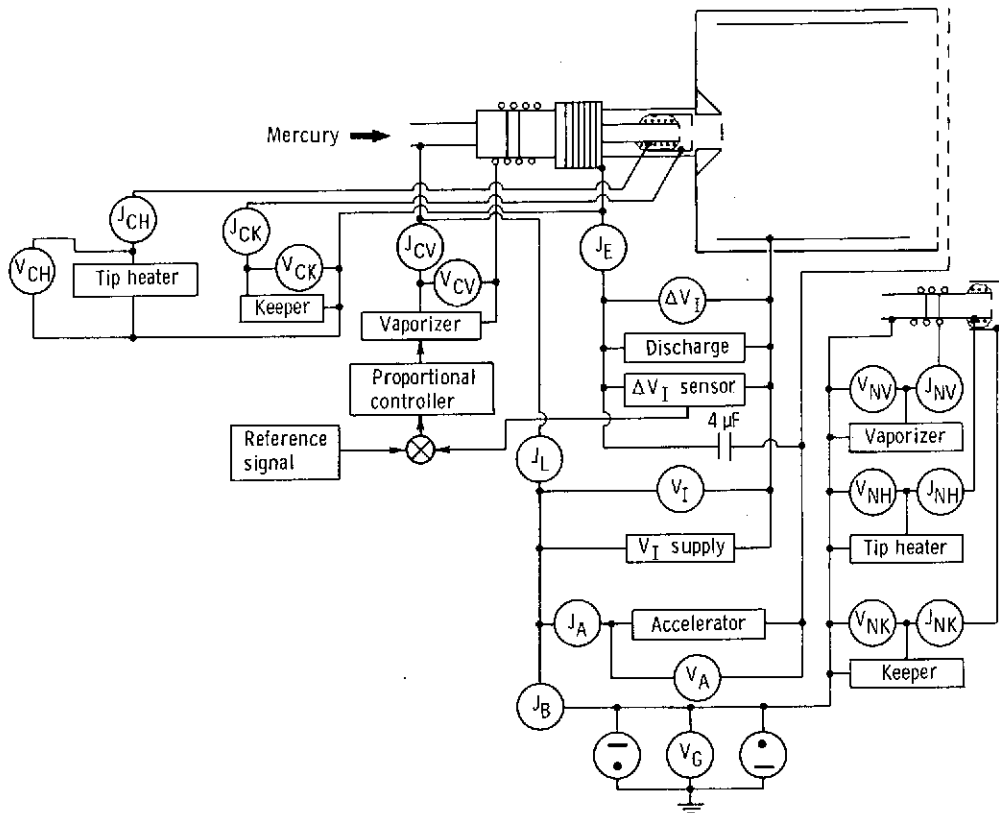
Figure 2. - Electrical circuit used for thruster testing. (See table II for definitions of symbols.)
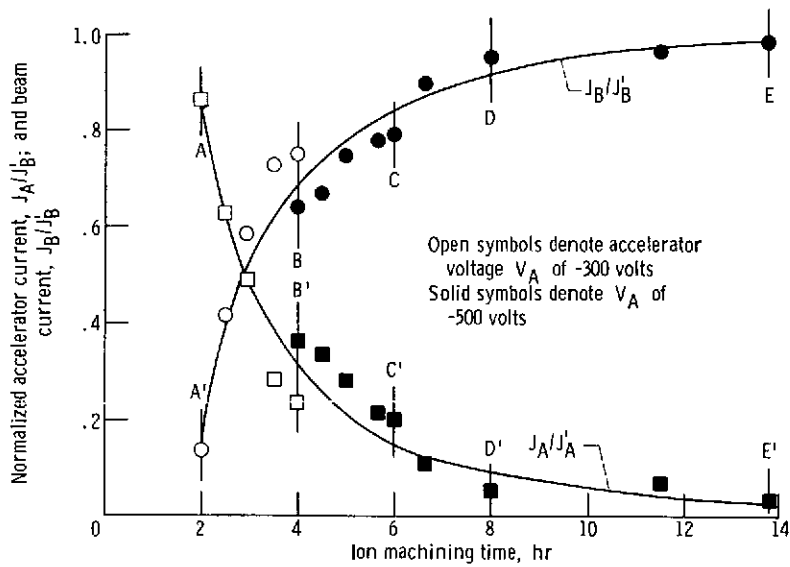
Figure 3. - Normalized accelerator current and normalized beam current as function of ion machining time, where J_B' is current measured on V_I supply. Net accelerating voltage, V_I, 1200 volts.
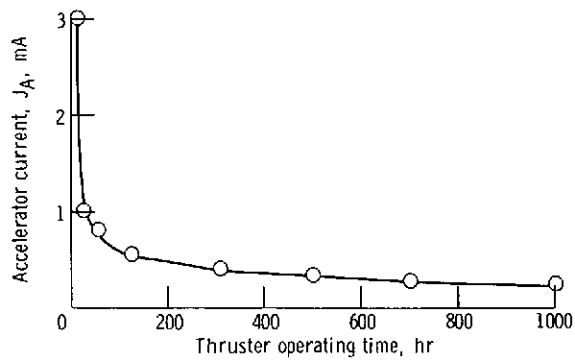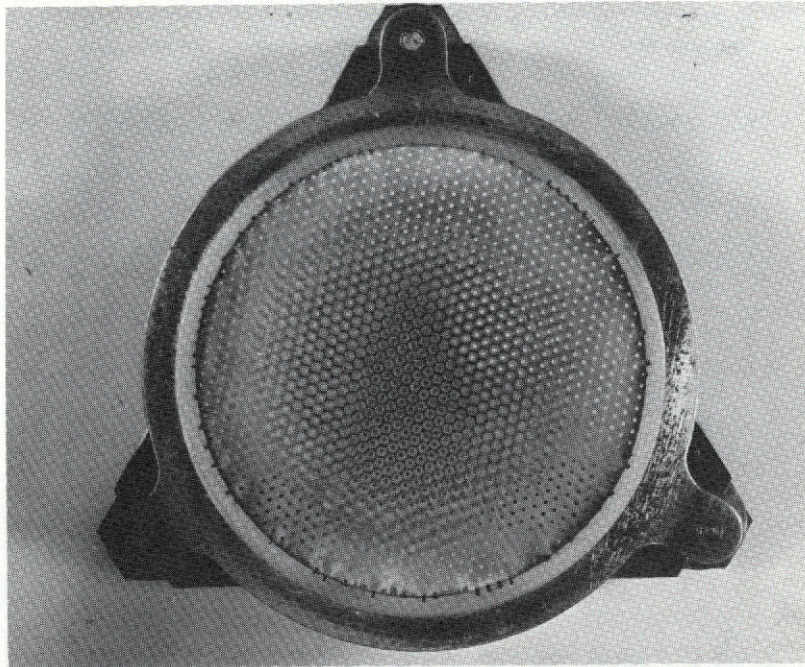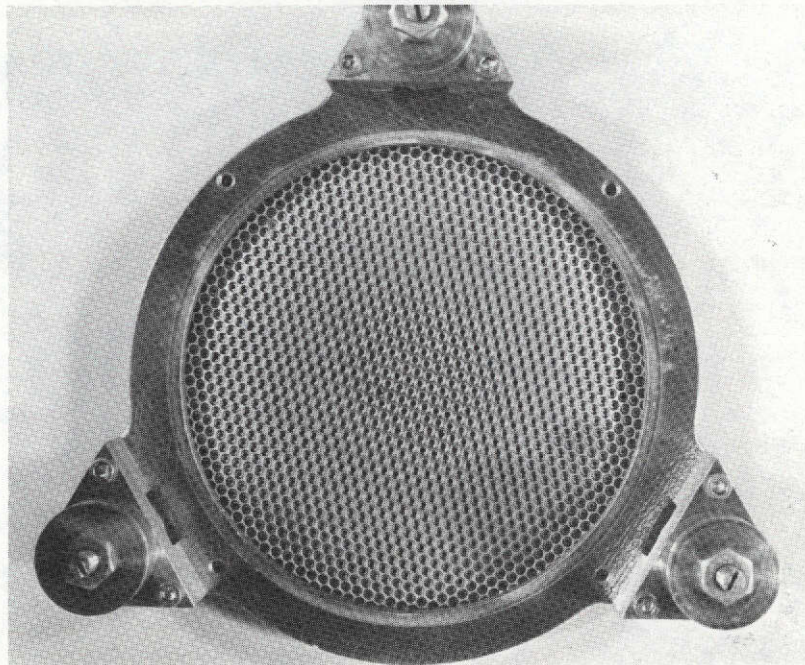

Figure 4. - Variation of accelerator current with thruster operating time.

14

Downstream face

Upstream face

Figure 5. - Upstream and downstream views of thruster grid assembly after 1006 hours of operation.
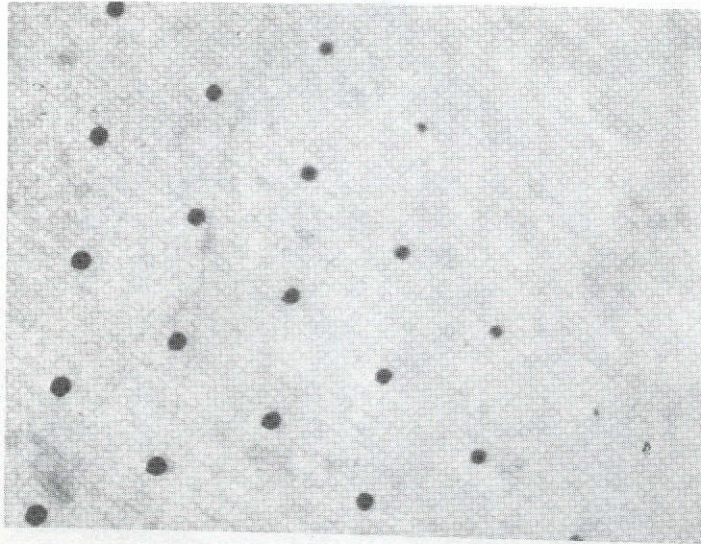
Figure 6. - Photomicrograph of downstream face of accelerator grid after 4 hours of ion machining.
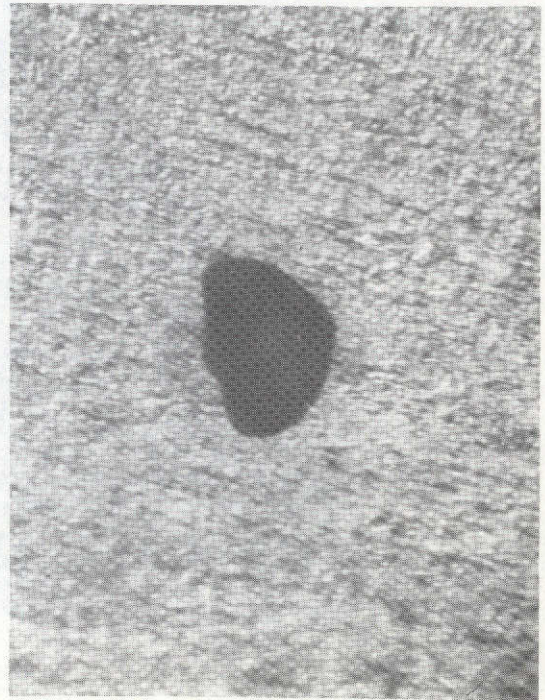
Figure 7. - Photomicrographs of partially sputtered-through accelerator hole viewed from downstream side of accelerator grid.
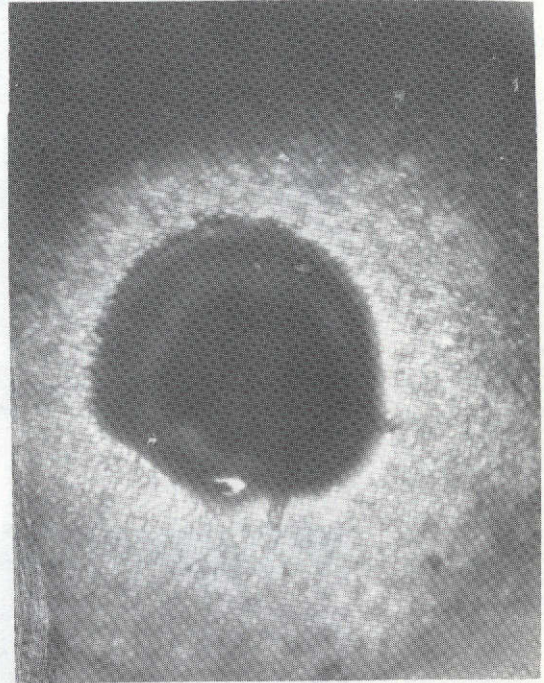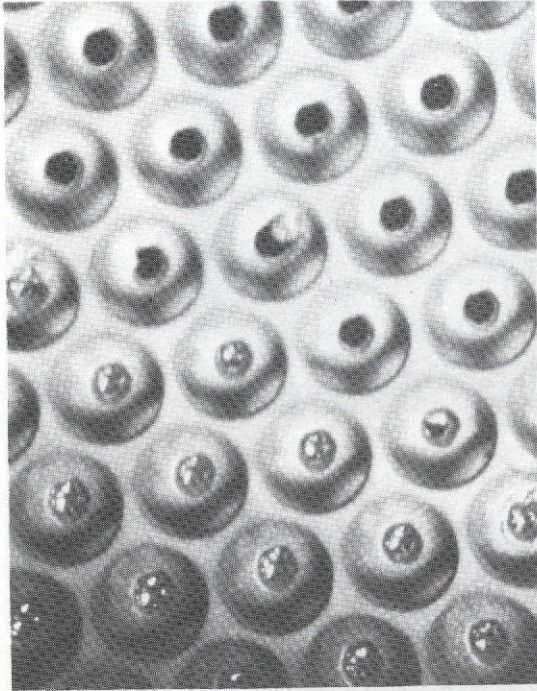
Figure 8. - Photomicrographs of partially sputtered-through accelerator holes viewed from upstream side of accelerator grid.
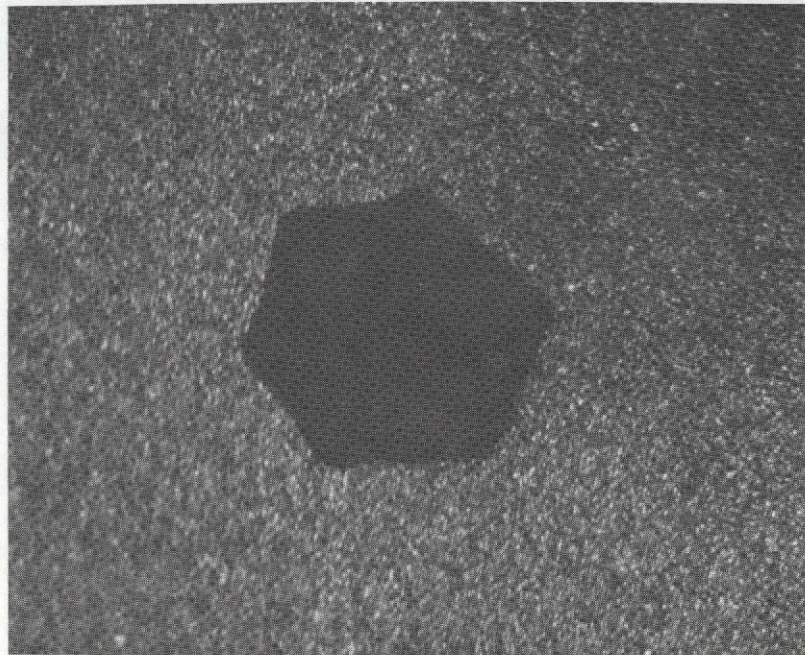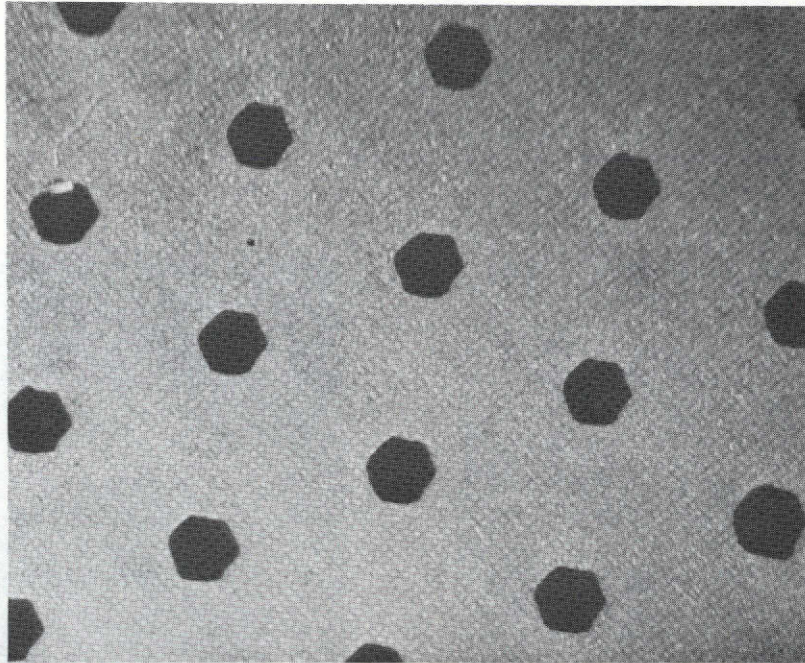
Figure 9. - Photomicrographs of hexagon accelerator hole geometry viewed from down-stream side of grid after 462 hours of operation.
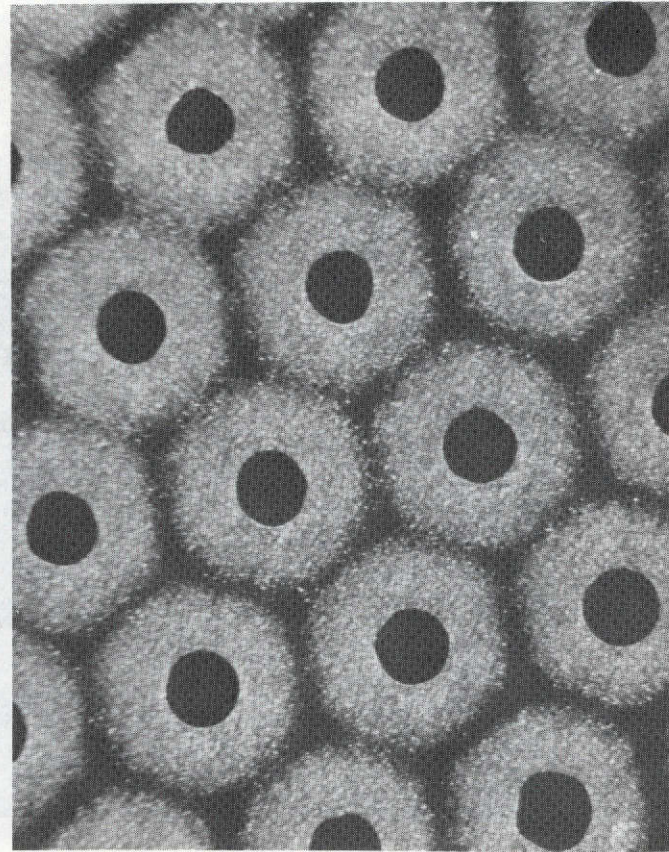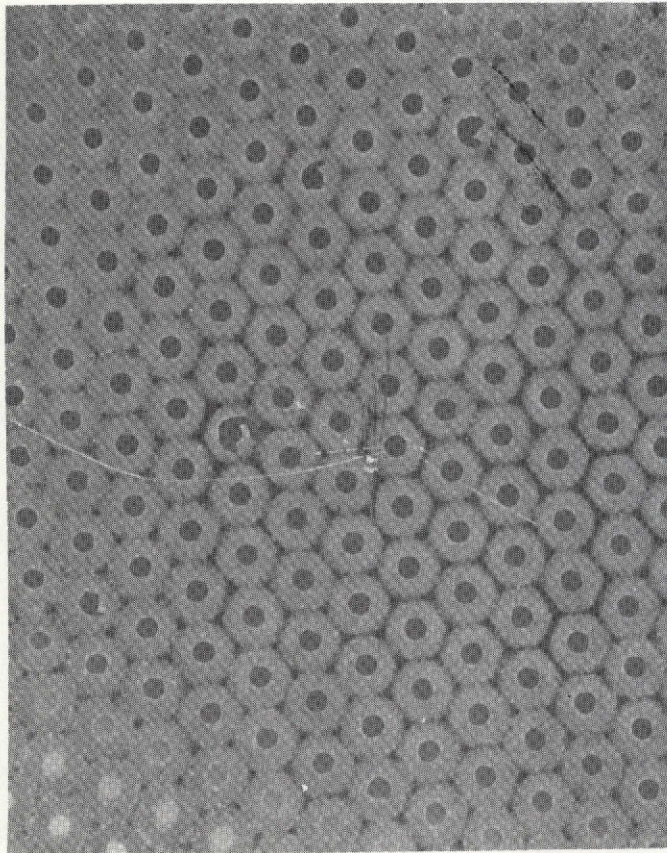
Figure 10. - Photomicrographs of charge exchange ion sputtering erosion patterns viewed from downstream side of accelerator grid after 462 hours of operation.
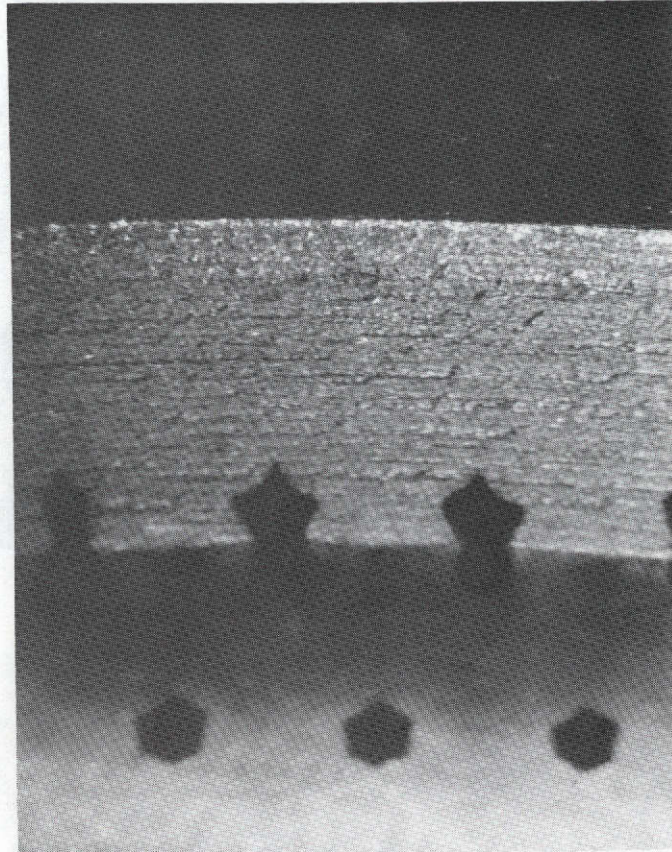
Figure 11. - Photomicrograph of sputtered grooves in accelerator grid mounting ring after 462 hours of operation.
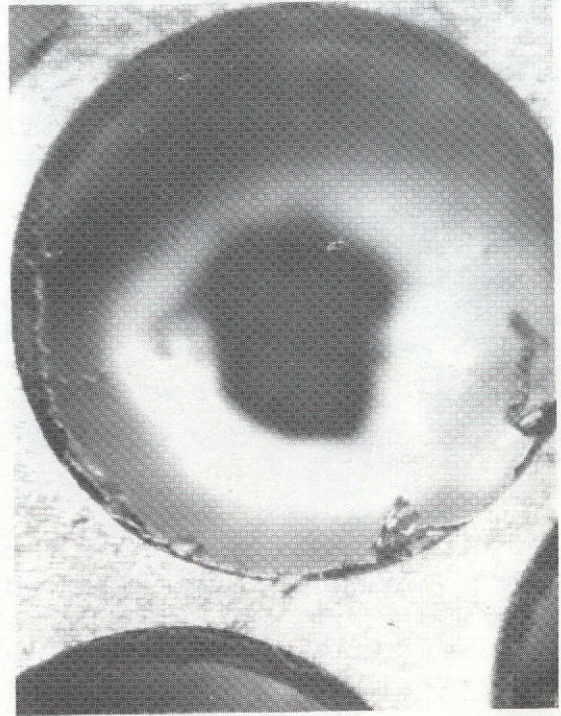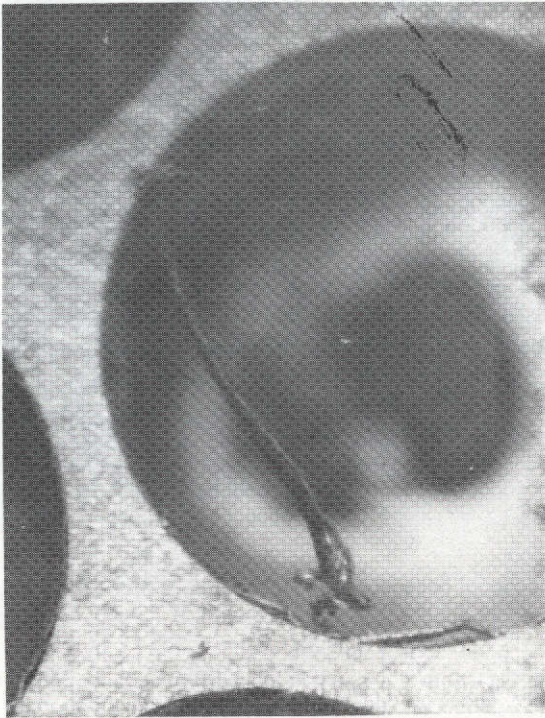
Figure 12. - Photomicrographs of deposition of sputtered accelerator grid material in screen holes after 20 hours of operation.
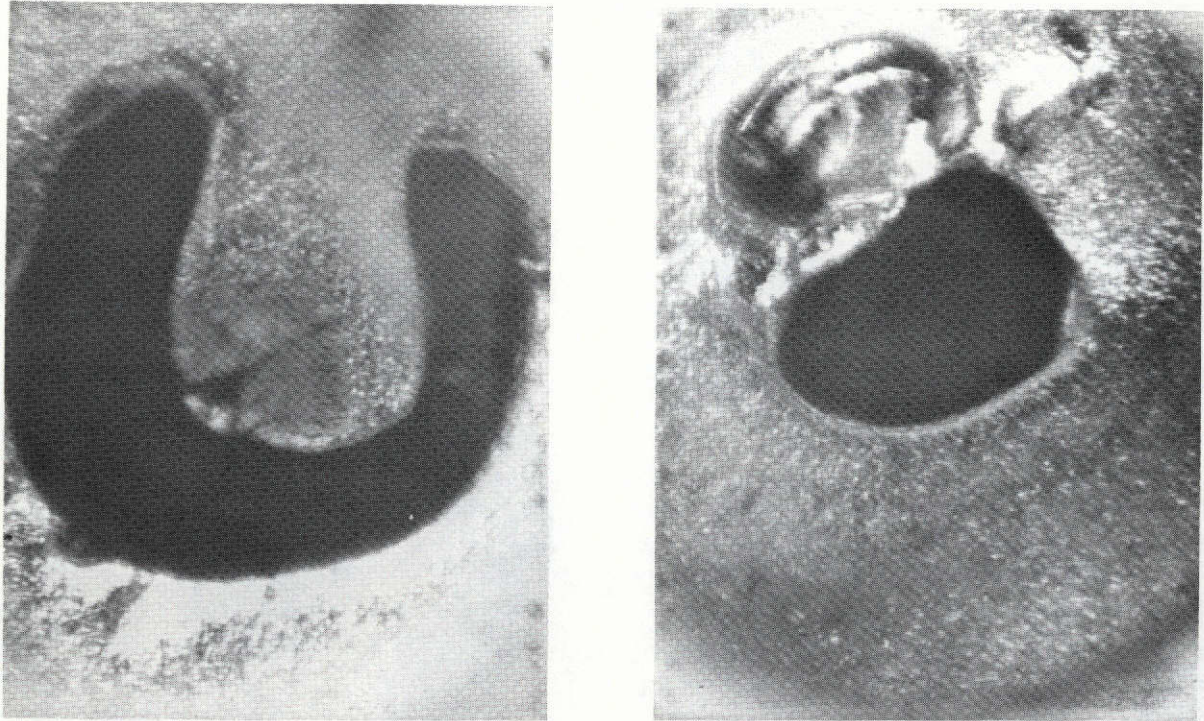
Figure 13. - Photomicrographs of distorted accelerator grid holes due to peeled flake on screen grid hole walls after 20 hours of operation.
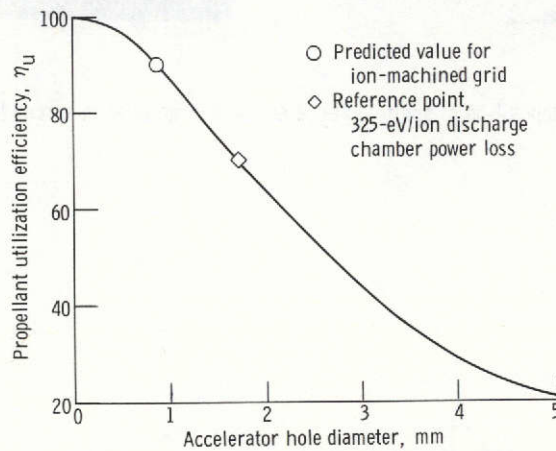

Figure 14. - Propellant utilization efficiency as function of accelerator hole diameter as predicted by equation (3), $\eta_u = 100/(1 + 0.149\ D^2)$. Reference point corresponds to η_u of 70 percent at discharge chamber loss of 325 eV/ion.

○ Small-hole accelerator grid (SHAG)
  after 149 hr of operation
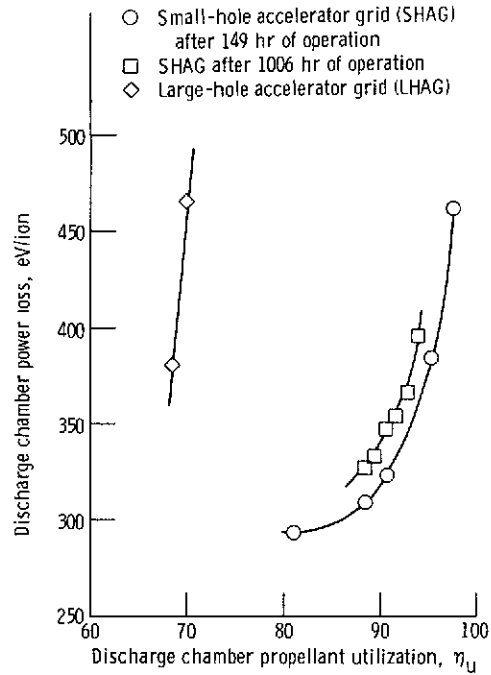□ SHAG after 1006 hr of operation
◇ Large-hole accelerator grid (LHAG)

Figure 15. – Discharge chamber power loss as
function of discharge chamber propellant
utilization for thruster with ion-machined
accelerator grid. Net accelerating voltage,
V_I, 1220 volts; accelerator voltage, V_A,
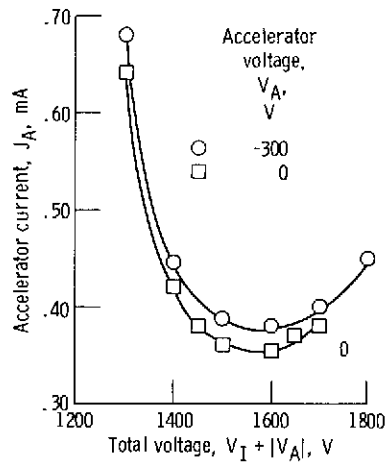-300 volts. (Data taken at constant mercury
flow.)

Figure 16. – Accelerator current
dependence on total voltage. Beam
current, J_B, 72 mA; propellant
utilization efficiency, η_u, 88.5
percent. (Data taken after 149 hr
of operation.)